Journal of Molecular Graphics and Modelling 55 (2015) 65–71

Contents lists available at ScienceDirect

Journal of Molecular Graphics and Modelling

journal homepage: www.elsevier.com/locate/JMGM

Short communication

Ab initio modeling approach towards establishing the structure and docking orientation of the *Porphyromonas gingivalis* FimA

Marni E. Cueno [a,*], Keiji Nagano [b], Kenichi Imai [a], Muneaki Tamura [a], Fuminobu Yoshimura [b], Kuniyasu Ochiai [a,*]

[a] Department of Microbiology, Nihon University, School of Dentistry, Tokyo 101-8310, Japan
[b] Department of Microbiology, School of Dentistry, Aichi Gakuin University, Nagoya 464-8650, Japan

ARTICLE INFO

Article history:
Accepted 7 November 2014
Available online 15 November 2014

Keywords:
Beta-sheet-rich
Epithelial cell-binding domain
FimA
Ab initio modeling
Porphyromonas gingivalis

ABSTRACT

Porphyromonas gingivalis FimA is a major aetiological agent in periodontal disease development, however, its structure has never been determined. Here, we established the mature *P. gingivalis* FimA ab initio model of all six FimA variants. We determined the conserved amino acid sequences of each FimA variant and generated mature FimA models. Subsequently, we validated their quality, protein empirical distribution, and radius of gyration. Similarly, structural comparison and topological orientation were elucidated, and the probable protein–protein docking was investigated. We found that the putative mature FimA model is β-sheet-rich and, likewise, we observed that each mature FimA model has varying levels of structural differences which can be topologically subdivided into the upper, middle, and lower FimA sections. Moreover, we found that the FimA epithelial cell-binding domain (EBD) is structurally conserved within the middle FimA section of all variants and FimA–FimA docking suggests that the FimA EBDs are oriented in opposite and alternating directions of each other.

1. Introduction

Porphyromonas gingivalis is a gram-negative black pigmented anaerobic bacterium that has been implicated as a major aetiological agent in the onset and progression of periodontal diseases by aggregating with other organisms in subgingival plaque biofilms and invading sulcular gingival epithelial cells which subsequently breaks down epithelial cell-to-cell junctions allowing the bacterium to further penetrate into deeper periodontal tissues and, likewise, colonize alveolar bone [1,2]. In addition, *P. gingivalis* possesses several potential virulence factors which include cysteine proteinases, hemagglutinins, liposaccharides, and fimbriae. Among the various virulence factors produced by this bacterium, fimbriae play a significant role [3].

P. gingivalis fimbriae are filamentous structures on the bacterial surface that are implicated in bacterial adherence to and colonization of host tissues [4–6]. It was previously reported that binding of *P. gingivalis* fimbriae to host cells is mediated by α5β1-integrins which triggers cell invasion via a cellular lipid raft [7,8]. At the molecular level, *P. gingivalis* fimbriae constitutes a predominant proinflammatory molecule which activates the Toll-like receptor (TLR) signaling pathway resulting in proinflammatory cytokine and chemokine induction [9,10], and upregulation of CD40, CD80, and CD86 [9]. Moreover, it was suggested that *P. gingivalis* fimbriae function as a pathogen-associated molecular pattern interacting with pattern-recognition receptors, like CD14 and CD11b/CD18, functioning as a recruiting receptor [9,11].

P. gingivalis fimbria has two distinct fimbrilin types, Mfa1 and FimA, with the latter playing an important role in host adhesion [6]. FimA proteins are positively and uniquely regulated by the FimS-FimR two-component system [12]. Similarly, FimA binds to varying eukaryotic proteins which includes, among others, saliva-derived proline-rich proteins [13], statherin [14], fibronectin, collagen, and laminin [15]. Previous studies have shown that *fimA*-deficient mutants lack the capability to invade human epithelial cells [16,17] highlighting the significance of FimA in host-bacterium interaction.

P. gingivalis fimA genes are classified into six genotypes (I, Ib, II, III, IV, V) based on varying virulence potential with each *P. gingivalis* strain containing a single distinct *fimA* gene [18–20]. This suggests that the structure of the FimA variants in each *P. gingivalis* strain differs. However, surprisingly no detailed FimA structural analyses have been reported thus far. A better structural understanding of the *P. gingivalis* FimA structural variants may contribute to the

* Corresponding authors at: Department of Microbiology, Nihon University School of Dentistry, 1-8-13 Kanda-Surugadai, Chiyoda-ku, Tokyo 101-8310, Japan. Tel.: +81 332198125.
E-mail addresses: marni.cueno@nihon-u.ac.jp (M.E. Cueno), ochiai.kuniyasu@nihon-u.ac.jp (K. Ochiai).

http://dx.doi.org/10.1016/j.jmgm.2014.11.001
1093-3263/

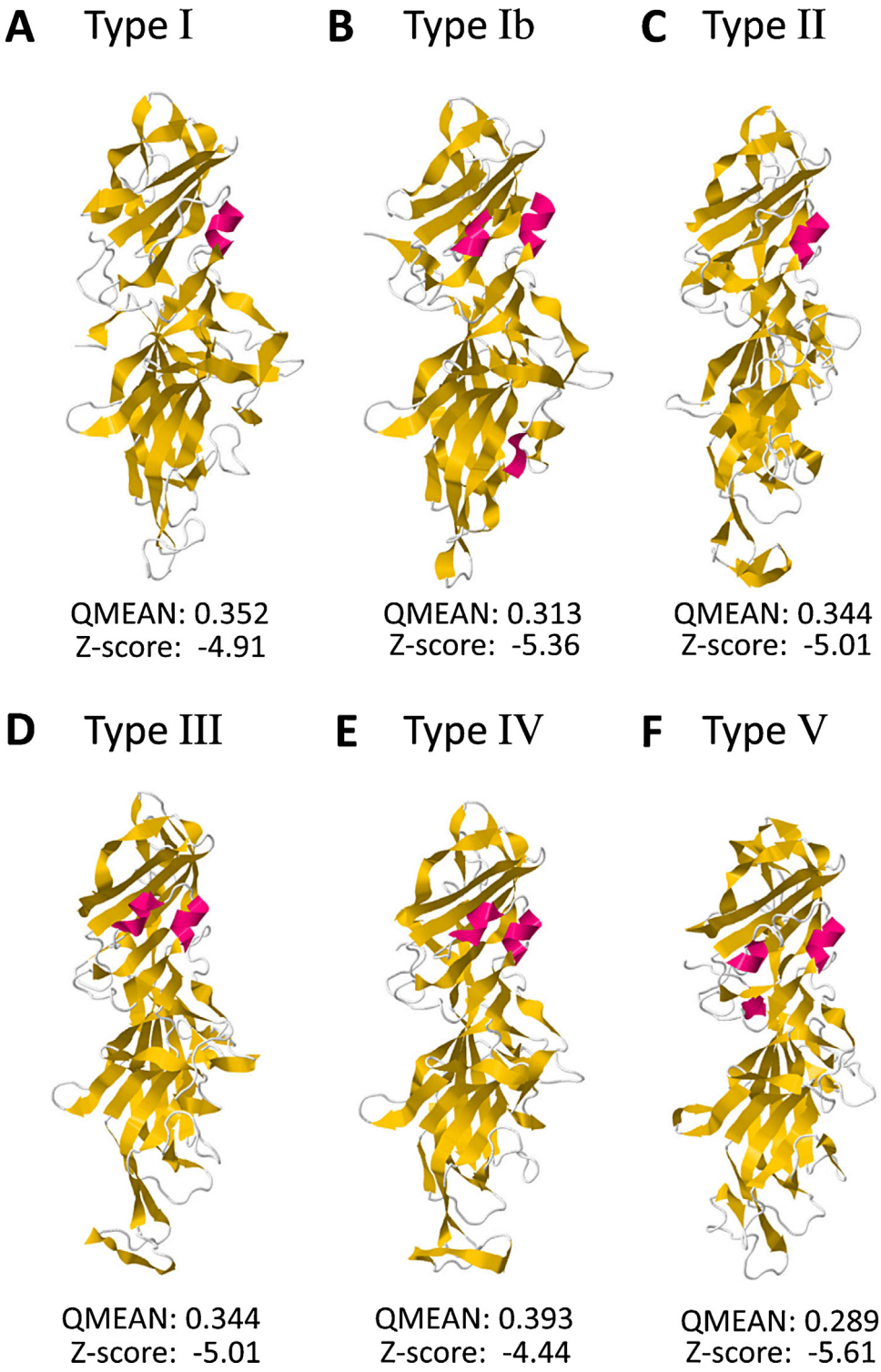

Fig. 1. Quality estimation of mature *P. gingivalis* FimA ab initio model variants generated. (A–F) Ribbon structure and model quality estimation of type I, Ib, II, III, IV, and V ab initio model variants, respectively. QMEAN and QMEAN *Z*-scores (*Z*-score) are indicated below. Ab initio models with QMEAN scores close to 0.3 and QMEAN *Z*-scores close to −5 were considered acceptable for further analyses. α-Helix (pink), β-sheets (yellow), and coils (white) are shown.

development of structure-based anti-bacterial therapies specifically targeting *P. gingivalis* FimA.

2. Materials and methods

2.1. Ab initio modeling and quality estimation

Throughout this study, we used FimA DNA sequences previously published and deposited in DDBJ [21]. Vector NTI (Life Technologies) was used to translate the DNA sequences to amino acid sequences which, subsequently, were used for multiple sequence alignment to establish the conserved amino acid sequences of each FimA variant. Phyre 2 server [22] was used to generate mature FimA ab initio models from the conserved amino acid sequences without the 46-amino acid-long peptide extensions found in the N-termini region [23–25]. Briefly, the Phyre server scans user-submitted sequences against the non-redundant

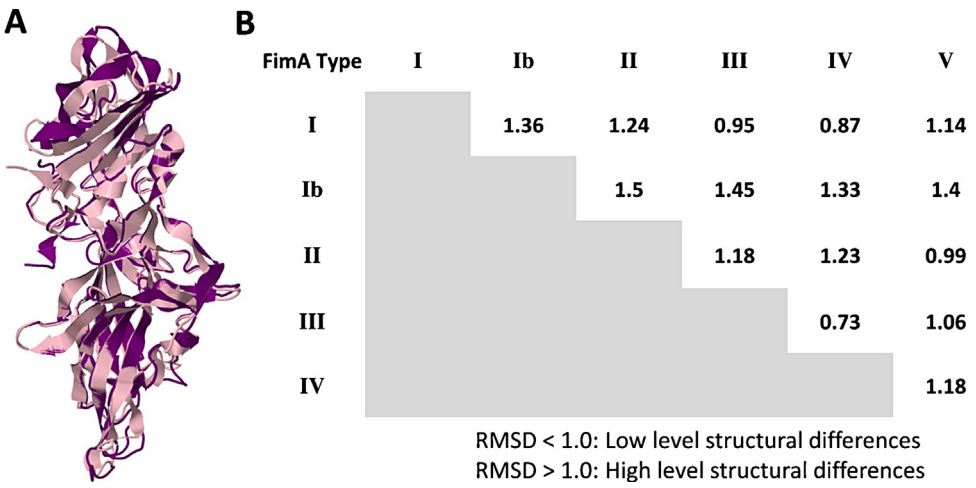

Fig. 2. *P. gingivalis* FimA ab initio models have varying levels of structural differences among variants. (A) Representative FimA ab initio model superimposition. FimA Type I (purple) and Ib (pink) ab initio models are indicated. (B) RMSD value comparison. RMSD values obtained after FimA ab initio model superimposition are indicated. RMSD values <1.0 indicate low level structural differences while RMSD values >1.0 indicate high level structural differences. All RMSD values are indicated in angstrom (Å). (For interpretation of the references to color in this figure legend, the reader is referred to the web version of the article.)

sequence database before constructing a profile. Secondary structures are predicted by three independent secondary structure prediction programs wherein the confidence values of each program are calculated and averaged. We validated the quality of the models using QMEAN (Qualitative Model Energy Analysis) and QMEAN *Z*-scores, whereby, QMEAN denotes the scoring function based on six terms of normalized potentials related to protein length and QMEAN *Z*-scores are estimates of the "degree of nativeness" observed in a generated model by describing the probability that a model is of comparable quality to known high-resolution protein structures [26]. We used the Jmol applet [27] to visualize the models.

2.2. Empirical distribution and coarse-grain molecular dynamics (CG-MD) simulation

Empirical distribution of amino acid residues found in each mature FimA model variant was determined by establishing the Ramachandran plot using RAMPAGE [28]. Briefly, the RAMPAGE server utilizes density-dependent smoothing of amino acid residues showing sharp boundaries at critical edges which would indicate a clear delineation between large empty areas and regions that are allowed but disfavored. Similarly, CG-MD was performed to determine the radius of gyration (R_{gyr}) of both the original and altered sialidase models using MDWeb [29]. Briefly, the MDWeb server is based on the original MDMoby software platform utilizing the Ambertools and VMD packages combined with in-house and publicly available programs. CG-MD simulation conditions were set at 1000 ps simulation time with Δt at 0.01 ps and output frequency collected at 10 ps.

2.3. Model superimposition and topology

FimA model superimposition was performed using SuperPose [30]. Briefly, SuperPose is composed of a front-end web interface written in Perl and HTML with a back-end for alignment, superposition, and Root Mean Square Deviation (RMSD) calculation. RMSD values of the superimposed Cα backbone close to 0 would indicate high structural similarity, whereas, RMSD values above 1 would insinuate high structural difference. Similarly, topological orientation of each mature FimA model variant was determined using PDBsum [31]. Briefly, topology diagrams representing the topological orientation of proteins illustrate how β-strands join up side-by-side to form β-sheets and how the α-helices are located within them. Arrow direction indicates the protein chain directionality, from the N- to the C-terminus, while the numbers within the secondary structural elements correspond to the residue numbering as indicated in the 3D protein structure. All RMSD values are indicated in angstrom (Å).

2.4. Protein–protein docking determination

We located the position of the probable conserved FimA epithelial cell-binding domain (EBD) in all models based on an earlier work [32] using Jmol. The EBD position was used as the basis to determine the probable FimA–FimA docking which ultimately would represent a simulated FimA oligomerization model. ClusPro 2.0 web server was used to establish protein–protein docking [33,34]. Briefly, ClusPro 2.0 is an accessible web server with an algorithm that first filters docked confirmations by selecting favorable desolvation and electrostatic properties, cluster structures using a hierarchical pairwise RMSD algorithm, and finally selects from among the most populated clusters. A total of 10 possible docking orientations are provided and considered for downstream analyses.

3. Results

3.1. *P. gingivalis* FimA is compact and β-sheet-rich

To determine the putative structure of each mature *P. gingivalis* FimA variant, ab initio modeling was performed. As seen in Fig. 1A–F (*upper panels*), visual inspection of the generated mature FimA models seem to suggest that a typical mature *P. gingivalis* FimA structure is mainly composed of β-sheets. In addition, we found that each putative mature FimA modeling variant generated has QMEAN scores close to 0.3 and QMEAN *Z*-scores close to −5 (Figs. 1A–F, *lower panels*). Given the low solvation and torsion angle energies of each putative mature FimA model (data not shown), we considered these values suitable for further analyses.

To further elucidate the quality and protein behavior of each FimA model, CG-MD simulation was performed in order to obtain the radius of gyration (R_{gyr}). We observed that each mature FimA model has low folding activity (Suppl. Fig. 1A) indicating that the generated models are stable and compact. To verify the structural composition of mature FimA proteins, empirical distribution of each mature FimA model was established. We observed that the

amino acid empirical distribution of each mature FimA model is generally found in the β-sheet conformation (Suppl. Fig. 1B) [35] consistent with our earlier observation.

3.2. Each P. gingivalis FimA variant has structural differences and similarities with other variants

To structurally compare each mature FimA model variant with those from other variants, model superimposition was conducted. Representative mature FimA model superimposition is shown (Fig. 2A) and RMSD scores of each model superimposition are tallied (Fig. 2B). Noticeably, superimposition between mature FimA model variants I and III; I and IV; II and V; and III and IV all have RMSD scores close to 1.0 indicating low level structural differences, whereas, other superimposition combinations showed RMSD scores >1.0 suggesting high level structural differences.

To further differentiate all six mature FimA model variants, predicted topological orientation of each mature FimA variant was established. Visual comparison of all FimA topology diagrams (Fig. 3A–F) suggests that there are FimA protein domains with both topological similarities and differences found in each mature FimA variant consistent with our earlier observations (Fig. 2B). We found that *P. gingivalis* FimA models of types I, Ib, III, and IV have 18 β-sheet conformations, whereas, types II and V have 16 and 17 β-sheet conformations, respectively. In addition, we observed a common topological orientation (Fig. 3, *dotted box*) and, using this as a reference point, we propose that the FimA protein topology can be subdivided into three sections (Fig. 3, *lower panel*) designated as: upper (left side of the common topological orientation), middle (common topological orientation in all variants), and lower (right side of the common topological orientation) sections. Noticeably, mature FimA model variants I and III (lower section); I and IV (lower section); II and V (upper section); and III and IV (both upper and lower sections) have similar topological orientations while FimA variant Ib have no similar topological orientation with other FimA variants consistent with RMSD scores (Fig. 2B).

3.3. FimA EBDs are oriented in opposite and alternating directions

To determine the possible FimA–FimA docking orientation, we determined the FimA EBD position in all FimA models. We found that the FimA EBD position has a similar location (middle section) in all FimA models (Suppl. Fig. 2 A–F) which may explain why all FimA proteins have this common section. Moreover, among the possible FimA–FimA docking orientations we obtained, we only considered probable protein docking orientations where the EBD is structurally accessible after protein docking since we believe that this is a vital structural prerequisite of the mature FimA protein [36]. In this regard, we found two probable docking orientations that places the FimA EBD in either a one-sided docking orientation (data not shown) or in opposite directions (Fig. 4A). To further elucidate which docking orientation favors FimA oligomerization, we docked a third FimA protein to these two possible FimA–FimA docking orientations. We found that the only possible docking orientation that would favor FimA oligomerization is when FimA EBD is oriented in alternate directions (Fig. 4B).

4. Discussion

P. gingivalis fimbriae has long been the focus of research in periodontal microbiology and pathogenesis [37], however, the FimA structure has never been determined while no protein with high homology to FimA has been found [38]. Throughout this computational study, we established that the mature *P. gingivalis* FimA models are compact and β-sheet-rich proteins consistent with a previous publication [39]. β-sheet-rich protein structures are

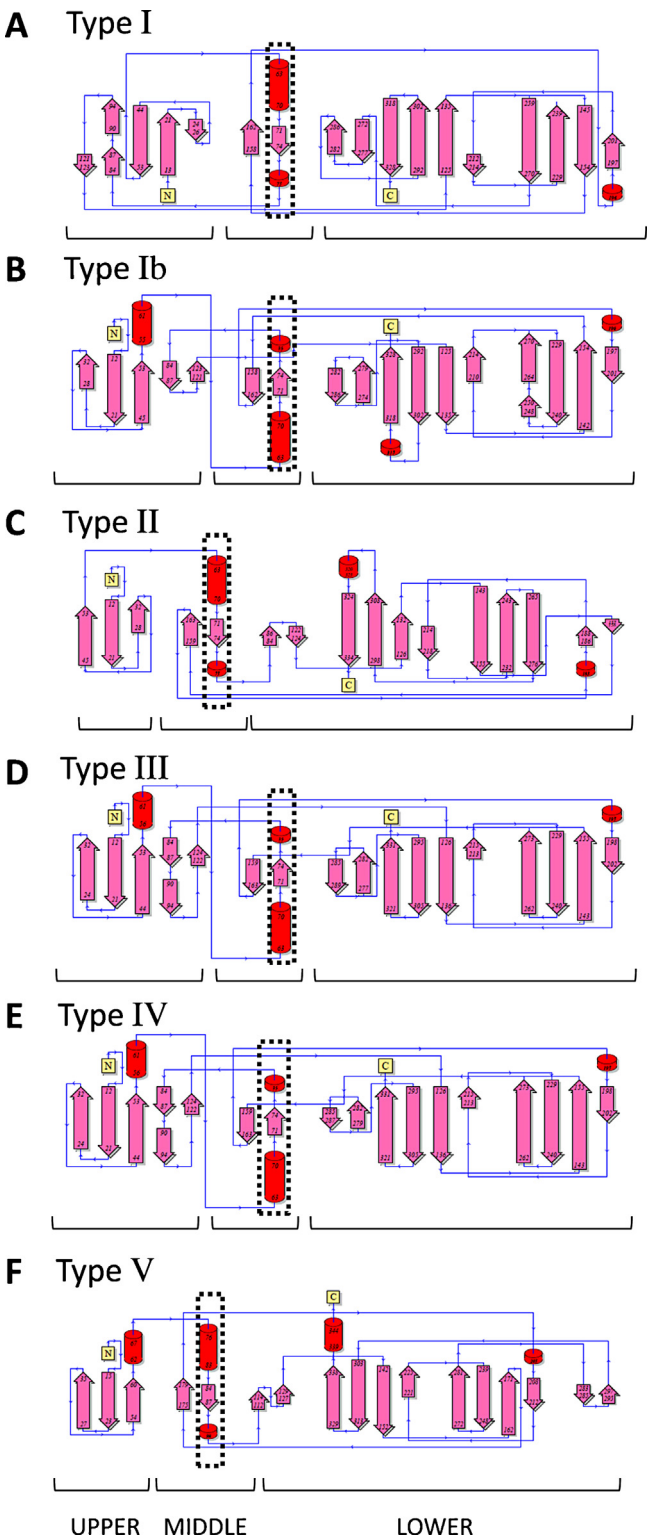

Fig. 3. Structural topology of each mature *P. gingivalis* FimA ab initio modeling variant. (A–F) Topological orientation of type I, Ib, II, III, IV, and V ab initio model variants, respectively. Coiled loops (violet line), β-sheets (pink arrow) and α-helices (red cylinders) are indicated. Common structural topology in all FimA ab initio modeling variants is boxed with dotted lines and designated as the proposed middle section as indicated below. Proposed upper and lower sections are likewise indicated below. (For interpretation of the references to color in this figure legend, the reader is referred to the web version of the article.)

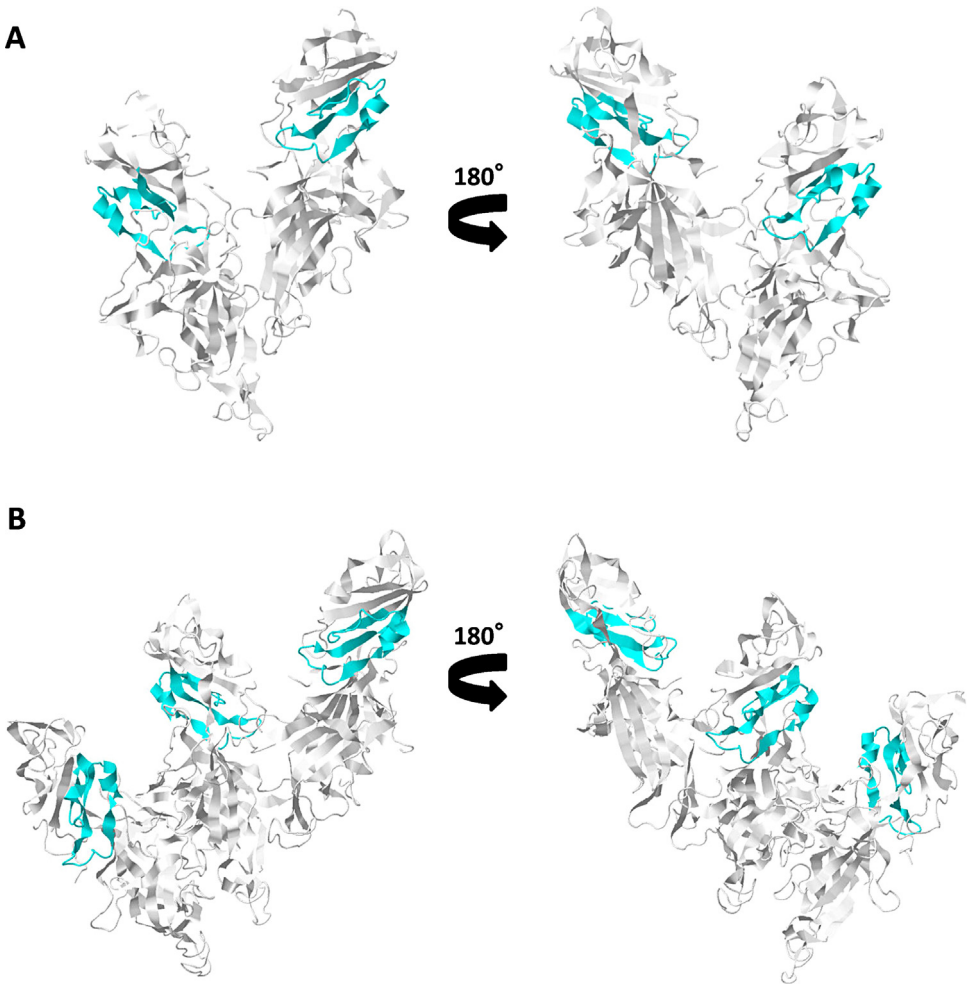

Fig. 4. *P. gingivalis* FimA epithelial cell-binding domain (EBD) is oriented in opposite and alternating direction. Protein docking of (A) two and (B) three FimA oligomers demonstrating the probable FimA oligomerization. (*Left and right panels*) Two opposite sides of FimA docking are shown. EBD position is indicated in blue. (For interpretation of the references to color in this figure legend, the reader is referred to the web version of the article.)

naturally and universally occurring protein structures that are accessible to polypeptide chains with greatly variegated amino acid sequences [40]. In addition, β-sheet-rich protein structures were revealed to have remarkable structural stability and mechanical resistance against various environmental factors [41–43] making such proteins insoluble and, thus, very difficult to obtain the structure using biophysical techniques [44,45]. This could explain why the *P. gingivalis* FimA structure has not been determined thus far and, likewise, may justify a computational approach (in this case ab initio modeling) towards determining the possible *P. gingivalis* FimA structure.

Additionally, we observed varying levels of structural differences among certain FimA ab initio model variants consistent with a previously published work, wherein, *P. gingivalis* FimA proteins are found to be antigenically heterogenous and have low-cross reactivity regardless of having identical amino acid sequences among variants. This was attributed to either preferential protein conformation or a discontinuous FimA polymer epitope [46]. Moreover, we found that certain superimposed FimA models do not share the same virulence potential which insinuates that FimA structural conformation have a lesser role in contributing to virulence consistent with previous works [3,5,47,48]. In addition, based on the topological similarities and differences visually observable among the FimA variants, we hypothesize that FimA undergoes preferential protein conformations in certain domains located in the variable upper and lower FimA sections that may influence physiological function.

All *P. gingivalis* strains, regardless of virulence, have the ability to adhere to epithelial cells [36] ascribable to the EBD [32] which would emphasize the structural significance of locating the EBD within the middle FimA section. It is also worth mentioning that although the EBD is located within the middle FimA section of all variants, types II, Ib, and IV have stronger infectious symptoms and inflammatory changes (mainly associated with virulence potential) as compared to types I, III, and V [20,49–51]. A previous work has demonstrated that FimA genotypes of *P. gingivalis* are not related to both adhesion and invasion to epithelial cells [36]. This implies that the EBD location is only related to adhesion and not to virulence. Furthermore, based on our simulated FimA oligomerization model, we propose that the probable FimA EBD orientation (opposite and alternating directions) could be important structural features that would contribute and maximize efficient epithelial cell adhesion.

5. Conclusion

In summary, we propose that *P. gingivalis* FimA is a compact and β-sheet-rich protein that can be topologically divided into three (upper, middle, lower) sections with the EBD located within the conserved middle FimA section and oriented to favor epithelial cell adhesion. Our results provide a better understanding of

the *P. gingivalis* FimA structure which we hope may contribute to the development of structure-based anti-bacterial therapies specifically targeting *P. gingivalis* FimA that could be utilized for the treatment of *P. gingivalis*-related periodontal diseases.

Acknowledgements

This work was supported by the following grants: Grants-in-Aid for Scientific Research, Nihon University President's Grant for Multidisciplinary Research, Satoh Fund and Dental Research Center-Nihon University School of Dentistry (Tokyo), "Strategic Research Base Development" Program for Private Universities subsidized by the Ministry of Education, Culture, Sports, Science and Technology (MEXT) 2010 (S1001024).

Appendix A. Supplementary data

Supplementary data associated with this article can be found, in the online version, at http://dx.doi.org/10.1016/j.jmgm.2014.11.001

References

[1] K. Tsuda, N. Furuta, H. Inaba, S. Kawai, K. Hanada, T. Yoshimori, et al., Functional analysis of alpha5beta1 integrin and lipid rafts in invasion of epithelial cells by *Porphyromonas gingivalis* using fluorescent beads coated with bacterial membrane vesicles, Cell Struct. Funct. 33 (2008) 123–132.
[2] O. Yilmaz, P. Verbeke, R.J. Lamont, D.M. Ojcius, Intercellular spreading of *Porphyromonas gingivalis* infection in primary gingival epithelial cells, Infect Immun. 74 (2006) 703–710.
[3] M. Enersen, K. Nakano, A. Amano, *Porphyromonas gingivalis* fimbriae, J. Oral Microbiol. 5 (2013).
[4] E. Andrian, D. Grenier, M. Rouabhia, *Porphyromonas gingivalis*-epithelial cell interactions in periodontitis, J. Dent. Res. 85 (2006) 392–403.
[5] C. Zheng, J. Wu, H. Xie, Differential expression and adherence of *Porphyromonas gingivalis* FimA genotypes, Mol. Oral Microbiol. 26 (2011) 388–395.
[6] F. Yoshimura, Y. Murakami, K. Nishikawa, Y. Hasegawa, S. Kawaminami, Surface components of *Porphyromonas gingivalis*, J. Periodontal Res. 44 (2009) 1–12.
[7] O. Yilmaz, K. Watanabe, R.J. Lamont, Involvement of integrins in fimbriae-mediated binding and invasion by *Porphyromonas gingivalis*, Cell Microbiol. 4 (2002) 305–314.
[8] R. Tamai, Y. Asai, T. Ogawa, Requirement for intercellular adhesion molecule 1 and caveolae in invasion of human oral epithelial cells by *Porphyromonas gingivalis*, Infect. Immun. 73 (2005) 6290–6298.
[9] G. Hajishengallis, H. Sojar, R.J. Genco, E. DeNardin, Intracellular signaling and cytokine induction upon interactions of *Porphyromonas gingivalis* fimbriae with pattern-recognition receptors, Immunol. Invest. 33 (2004) 157–172.
[10] G. Hajishengallis, M. Wang, S. Liang, Induction of distinct TLR2-mediated proinflammatory and proadhesive signaling pathways in response to *Porphyromonas gingivalis* fimbriae, J. Immunol. 182 (2009) 6690–6696.
[11] G. Hajishengallis, R.I. Tapping, E. Harokopakis, S. Nishiyama, P. Ratti, R.E. Schifferle, et al., Differential interactions of fimbriae and lipopolysaccharide from *Porphyromonas gingivalis* with the Toll-like receptor 2-centred pattern recognition apparatus, Cell. Microbiol. 8 (2006) 1557–1570.
[12] K. Nishikawa, M.J. Duncan, Histidine kinase-mediated production and autoassembly of *Porphyromonas gingivalis* fimbriae, J. Bacteriol. 192 (2010) 1975–1987.
[13] A. Amano, T. Nakamura, S. Kimura, I. Morisaki, I. Nakagawa, S. Kawabata, et al., Molecular interactions of *Porphyromonas gingivalis* fimbriae with host proteins: kinetic analyses based on surface plasmon resonance, Infect. Immun. 67 (1999) 2399–2405.
[14] A. Amano, K. Kataoka, P.A. Raj, R.J. Genco, S. Shizukuishi, Binding sites of salivary statherin for *Porphyromonas gingivalis* recombinant fimbrillin, Infect. Immun. 64 (1996) 4249–4254.
[15] S. Hamada, A. Amano, S. Kimura, I. Nakagawa, S. Kawabata, I. Morisaki, The importance of fimbriae in the virulence and ecology of some oral bacteria, Oral Microbiol. Immunol. 13 (1998) 129–138.
[16] T. Njoroge, R.J. Genco, H.T. Sojar, N. Hamada, C.A. Genco, A role for fimbriae in *Porphyromonas gingivalis* invasion of oral epithelial cells, Infect. Immun. 65 (1997) 1980–1984.
[17] A. Weinberg, C.M. Belton, Y. Park, R.J. Lamont, Role of fimbriae in *Porphyromonas gingivalis* invasion of gingival epithelial cells, Infect. Immun. 65 (1997) 313–316.
[18] A. Amano, I. Nakagawa, K. Kataoka, I. Morisaki, S. Hamada, Distribution of *Porphyromonas gingivalis* strains with fimA genotypes in periodontitis patients, J. Clin. Microbiol. 37 (1999) 1426–1430.
[19] T. Kato, S. Kawai, K. Nakano, H. Inaba, M. Kuboniwa, I. Nakagawa, et al., Virulence of *Porphyromonas gingivalis* is altered by substitution of fimbria gene with different genotype, Cell. Microbiol. 9 (2007) 753–765.
[20] A. Amano, I. Nakagawa, N. Okahashi, N. Hamada, Variations of *Porphyromonas gingivalis* fimbriae in relation to microbial pathogenesis, J. Periodontal. Res. 39 (2004) 136–142.
[21] K. Nagano, Y. Abiko, Y. Yoshida, F. Yoshimura, Genetic and antigenic analyses of *Porphyromonas gingivalis* FimA fimbriae, Mol. Oral Microbiol. 28 (2013) 392–403.
[22] L.A. Kelley, M.J. Sternberg, Protein structure prediction on the Web: a case study using the Phyre server, Nat. Protoc. 4 (2009) 363–371.
[23] T. Kadowaki, K. Nakayama, F. Yoshimura, K. Okamoto, N. Abe, K. Yamamoto, Arg-gingipain acts as a major processing enzyme for various cell surface proteins in *Porphyromonas gingivalis*, J. Biol. Chem. 273 (1998) 29072–29076.
[24] M. Shoji, A. Yoshimura, H. Yoshioka, A. Takade, Y. Takuma, H. Yukitake, et al., Recombinant *Porphyromonas gingivalis* FimA preproprotein expressed in *Escherichia coli* is lipidated and the mature or processed recombinant FimA protein forms a short filament in vitro, Can. J. Microbiol. 56 (2010) 959–967.
[25] K. Nakayama, F. Yoshimura, T. Kadowaki, K. Yamamoto, Involvement of arginine-specific cysteine proteinase (Arg-gingipain) in fimbriation of *Porphyromonas gingivalis*, J. Bacteriol. 178 (1996) 2818–2824.
[26] P. Benkert, M. Biasini, T. Schwede, Toward the estimation of the absolute quality of individual protein structure models, Bioinformatics 27 (2011) 343–350.
[27] A. Herraez, Biomolecules in the computer: Jmol to the rescue, Biochem. Mol. Biol. Educ. 34 (2006) 255–261.
[28] S.C. Lovell, I.W. Davis, W.B. Arendall 3rd, P.I. de Bakker, J.M. Word, M.G. Prisant, et al., Structure validation by Calpha geometry: phi, psi and Cbeta deviation, Proteins 50 (2003) 437–450.
[29] A. Hospital, P. Andrio, C. Fenollosa, D. Cicin-Sain, M. Orozco, J.L. Gelpi, MDWeb and MDMoby: an integrated web-based platform for molecular dynamics simulations, Bioinformatics 28 (2012) 1278–1279.
[30] R. Maiti, G.H. Van Domselaar, H. Zhang, D.S. Wishart, SuperPose: a simple server for sophisticated structural superposition, Nucleic Acids Res. 32 (2004) W590–W594.
[31] R.A. Laskowski, PDBsum: summaries and analyses of PDB structures, Nucleic Acids Res. 29 (2001) 221–222.
[32] H.T. Sojar, Y. Han, N. Hamada, A. Sharma, R.J. Genco, Role of the amino-terminal region of *Porphyromonas gingivalis* fimbriae in adherence to epithelial cells, Infect. Immun. 67 (1999) 6173–6176.
[33] S.R. Comeau, D.W. Gatchell, S. Vajda, C.J. Camacho, ClusPro: a fully automated algorithm for protein–protein docking, Nucleic Acids Res. 32 (2004) W96–W99.
[34] S.R. Comeau, D.W. Gatchell, S. Vajda, C.J. Camacho, ClusPro: an automated docking and discrimination method for the prediction of protein complexes, Bioinformatics 20 (2004) 45–50.
[35] C.M. Deane, F.H. Allen, R. Taylor, T.L. Blundell, Carbonyl–carbonyl interactions stabilize the partially allowed Ramachandran conformations of asparagine and aspartic acid, Protein Eng. 12 (1999) 1025–1028.
[36] J.E. Umeda, C. Missailidis, P.L. Longo, D. Anzai, M. Wikstrom, M.P. Mayer, Adhesion and invasion to epithelial cells by fimA genotypes of *Porphyromonas gingivalis*, Oral Microbiol. Immunol. 21 (2006) 415–419.
[37] J. Slots, R.J. Gibbons, Attachment of *Bacteroides melaninogenicus* subsp. asaccharolyticus to oral surfaces and its possible role in colonization of the mouth and of periodontal pockets, Infect. Immun. 19 (1978) 254–264.
[38] M. Enersen, I. Olsen, O. Kvalheim, D.A. Caugant, FimA genotypes and multilocus sequence types of *Porphyromonas gingivalis* from patients with periodontitis, J. Clin. Microbiol. 46 (2008) 31–42.
[39] F. Yoshimura, T. Takasawa, M. Yoneyama, T. Yamaguchi, H. Shiokawa, T. Suzuki, Fimbriae from the oral anaerobe bacteroides-gingivalis – physical, chemical, and immunological properties, J. Bacteriol. 163 (1985) 730–734.
[40] C.E. MacPhee, C.M. Dobson, Formation of mixed fibrils demonstrates the generic nature and potential utility of amyloid nanostructures, J. Am. Chem. Soc. 122 (2000) 12707–12713.
[41] I. Krasnov, I. Diddens, N. Hauptmann, G. Helms, M. Ogurreck, T. Seydel, et al., Mechanical properties of silk: Interplay of deformation on macroscopic and molecular length scales, Phys. Rev. Lett. 100 (2008).
[42] S. Keten, J.F.R. Alvarado, S. Muftu, M.J. Buehler, Nanomechanical characterization of the triple beta-helix domain in the cell puncture needle of bacteriophage T4 virus, Cell. Mol. Bioeng. 2 (2009) 66–74.
[43] J.F. Smith, T.P.J. Knowles, C.M. Dobson, C.E. MacPhee, M.E. Welland, Characterization of the nanoscale properties of individual amyloid fibrils, Proc. Natl. Acad. Sci. U. S. A. 103 (2006) 15806–15811.
[44] K. Makabe, D. McElheny, V. Tereshko, A. Hilyard, G. Gawlak, S. Yan, et al., Atomic structures of peptide self-assembly mimics, Proc. Natl. Acad. Sci. U. S. A. 103 (2006) 17753–17758.
[45] N. Benseny-Cases, M. Cocera, J. Cladera, Conversion of non-fibrillar beta-sheet oligomers into amyloid fibrils in Alzheimer's disease amyloid peptide aggregation, Biochem. Biophys. Res. Commun. 361 (2007) 916–921.
[46] K. Nagano, Y. Hasegawa, Y. Abiko, Y. Yoshida, Y. Murakami, F. Yoshimura, *Porphyromonas gingivalis* FimA fimbriae: fimbrial assembly by fimA alone in the fim gene cluster and differential antigenicity among fimA genotypes, PLoS ONE 7 (2012) e43722.
[47] T. Beikler, U. Peters, S. Prajaneh, K. Prior, B. Ehmke, T.F. Flemmig, Prevalence of *Porphyromonas gingivalis* fimA genotypes in Caucasians, Eur. J. Oral Sci. 111 (2003) 390–394.
[48] P.J. Perez-Chaparro, A. Rouillon, J. Minet, G.I. Lafaurie, M. Bonnaure-Mallet, FimA genotypes and PFGE profile patterns in *Porphyromonas gingivalis* isolates from subjects with periodontitis, Oral Microbiol. Immunol. 24 (2009) 423–426.
[49] A. Amano, M. Kuboniwa, I. Nakagawa, S. Akiyama, I. Morisaki, S. Hamada, Prevalence of specific genotypes of *Porphyromonas gingivalis* fimA and periodontal health status, J. Dent. Res. 79 (2000) 1664–1668.

[50] K. Nakano, M. Kuboniwa, I. Nakagawa, T. Yamamura, R. Nomura, N. Okahashi, et al., Comparison of inflammatory changes caused by *Porphyromonas gingivalis* with distinct fimA genotypes in a mouse abscess model, Oral Microbiol. Immunol. 19 (2004) 205–209.

[51] I. Nakagawa, A. Amano, M. Kuboniwa, T. Nakamura, S. Kawabata, S. Hamada, Functional differences among FimA variants of *Porphyromonas gingivalis* and their effects on adhesion to and invasion of human epithelial cells, Infect. Immun. 70 (2002) 277–285.